Korean J. Chem. Eng., **28**(2), 348-356 (2011)
DOI: 10.1007/s11814-010-0364-7

Study of the structural characteristics of a divided wall column using the sloppy distillation arrangement

Senug Hyun Lee*, Mohammad Shamsuzzoha*, Myungwan Han, Young Han Kim***, and Moonyong Lee*,†**

*School of Chem. Eng. & Tech. Yeungnam University, 214-1 Dae-dong, Gyeongsan, Gyeongbuk 712-749 Korea
**Department of Chemical Engineering, Chungnam National University, Daejeon 305-764, Korea
***Department of Chemical Engineering, Dong-A University, 840 Hadan-dong, Saha-gu, Busan 604-714, Korea
(*Received 24 May 2010 • accepted 19 June 2010*)

Abstract−An efficient design method is proposed for determining the optimal design structure of a dividing wall column (DWC). The internal section of the DWC is divided into four separate sections and matched to the sloppy arrangement with three conventional simple columns. The light and heavy key component mole-fractions are used as the design variables in each column. The structure that gives superior energy efficiency in the shortcut sloppy case also brings superior energy efficiency in the DWC, while the optimal internal flow distribution of the DWC is different from that obtained from the sloppy configuration. Based upon an extensive simulation study, a two-step approach is proposed for the DWC design: the optimal DWC structure is first determined by applying the shortcut method to the sloppy configuration; the optimal internal flow distribution is then found from the corresponding DWC configuration. The simulation study shows that the DWC designed by the proposed method gives a near-optimal structure.

Key words: Divided Wall Column, Thermally Coupled Distillation Column, Optimal Structure Design, Energy Efficiency, Shortcut Design Method

INTRODUCTION

Distillation is predominantly used for liquid separation, driving nearly all other separation techniques out of the process industry. The huge impact of distillation processes both on operation and investment costs has motivated the development of various types of fully thermally coupled distillation columns (FTCDC) that can usher in savings in energy and capital cost [1-19]. In particular, the divided wall column (DWC) has gained wide acceptance as an efficient means to implement the fully thermally coupled configuration and has thus rapidly expanded its commercial application. In the separation of ternary mixtures, the DWC possesses a significant advantage in energy savings by avoiding the remixing problem that occurs in a conventional sequential two-column system. The DWC also significantly reduces space and investment requirements over conventional distillation configurations.

Despite the high potential of the DWC economic benefits, a lack of reliable design methods has prevented their commercial application. In DWCs, the entire separation task occurs in one thermally coupled column shell, which makes for a much more difficult design structure compared to conventional distillation columns. Accordingly, several studies have been conducted to address the DWC design structure. Triantafyllou and Smith [20] proposed an FTCDC design using a three-column model. The method provides a good basis for investigating the degrees of freedom and the number of trays in an easy manner; however, it requires trial-error steps for matching the compositions of the interlinking streams. Amminudin et al. [21] developed a semi-rigorous method for the initial design of an FTCDC based on the concept of equilibrium stage composition. In their study, the FTCDC was divided into two separate columns to eliminate interlinking and obtain an optimal initial design that could be confirmed through rigorous simulation. Agrawal and Fidkowski [22] simplified the FTCDC structural design by eliminating one interconnection between the prefractionator and mainfractionator. Subsequently, Kim [8] also proposed a method for the FTCDC structural design based on the observation that when a portion of the mid-boiling component was dominant, the number of trays in the prefractionator was closer to that of the mid-section in the mainfractionator. Premkumar and Rangaiah [23] utilized a three-column configuration for the initial design structure of the DWC in their study for the retrofit of a conventional column system to a DWC. The initial structure obtained by a shortcut was then optimized in a rigorous simulation step.

In fact, once a product purity required is given for a DWC, the optimal structure and internal traffics should be determined primarily by feed characteristics. Furthermore, the similarity between the DWC and the corresponding conventional column configurations can also largely vary with the feed mixture type. Most of the previous studies investigated a specific feed mixture and, thus, the results were restricted to that particular feed rather than a general one. It remains unclear how the main design variables affect the overall performance of the DWC. Furthermore, many existing methods require a complex and iterative calculation step for determining the column structure. Therefore, it is still a challenging task for practical engineers to determine near-optimal design conditions for the DWC in a simple and efficient manner in the initial design stage.

In this paper, a shortcut method is proposed for determining the DWC structure, including the location of the feed tray, the side-stream tray, and the divided wall section, as well as the total number of trays

†To whom correspondence should be addressed.
E-mail: mynlee@yu.ac.kr

in each main and pre-fractionation section. The proposed method utilizes the classical Fenske-Underwood-Gilliland method, widely used in the initial design structure of the conventional distillation columns, by applying it on a sloppy column configuration with three conventional simple columns that is structurally equivalent to the DWC. The feed mixtures belonging to ideal solutions were evaluated and classified into nine cases based upon relative volatility and composition of the key components. To investigate the sensitivity and consistency of the optimal structure and internal flows, energy consumption for each feed mixture case was analyzed and compared to four different simulation cases.

STRUCTURAL SIMILARITY BETWEEN DWC AND SLOPPY CONFIGURATIONS

Fig. 1 compares a DWC and a sloppy column configuration for ternary mixture separation. From Fig. 1, as noted by Amminudin et al. [21], it is apparent that the pre-fractionation section and the upper and lower parts of the main-fractionation section in the DWC are equivalent to the split column and the light and the heavy end column in the sloppy configuration, respectively.

In the sloppy column configuration, the ternary mixture feed is first fed into the split column for pre-fractionation and separated into light and heavy components. The intermediate component is distributed to both the top and bottom of the split column. The mixture of light and intermediate components from the overhead of the split column is then fed into the light end column and separated into pure light and intermediate component products. The mixture of heavy and intermediate components from the bottom of the split column is fed to the heavy end column and separated to pure heavy and intermediate component products.

In the DWC, the ternary mixture feed is fed to the pre-fractionation section and separated into light and heavy components. The intermediate component is distributed to both the top and bottom of the pre-fractionation section. The mixture of light and intermediate components from the top of the pre-fractionation section enters into the main-fractionation section and is separated in its upper part (or the section between the top product and side product streams). The mixture of heavy and intermediate components from the bottom of the pre-fractionation section is then fed into the main-fractionation section and separated in the lower part of the main-fractionation section (or the section between the side product and bottom product streams).

One of the main differences between the DWC and the sloppy configuration is the energy source for generating the internal flows; in the DWC, the liquid and vapor flows in the pre-fractionation section utilize those from the main-fractionation section in a thermally-coupled manner, while in the sloppy configuration, the liquid and vapor flows in the split column are provided by the external condenser and reboiler of the split column, respectively. Furthermore, in the DWC, the liquid and vapor flows from the side product tray utilize the internal flows, while in the sloppy configuration, the corresponding liquid and vapor flows from the top of the heavy end column and from the bottom of the light end column are generated by the external condenser of the heavy end column and the external reboiler of the light end column, respectively. With the exception of this thermally-coupled feature, the sloppy configuration is structurally equivalent to the DWC in that each column in the sloppy configuration is rigorously matched with each corresponding section in the DWC in terms of its function in separation. Based on this structural similarity, the initial estimates of the DWC structure can be easily determined by applying the existing shortcut design methods that are used for the conventional distillation columns to the equivalent sloppy configuration. In this study, a well-known Fen-

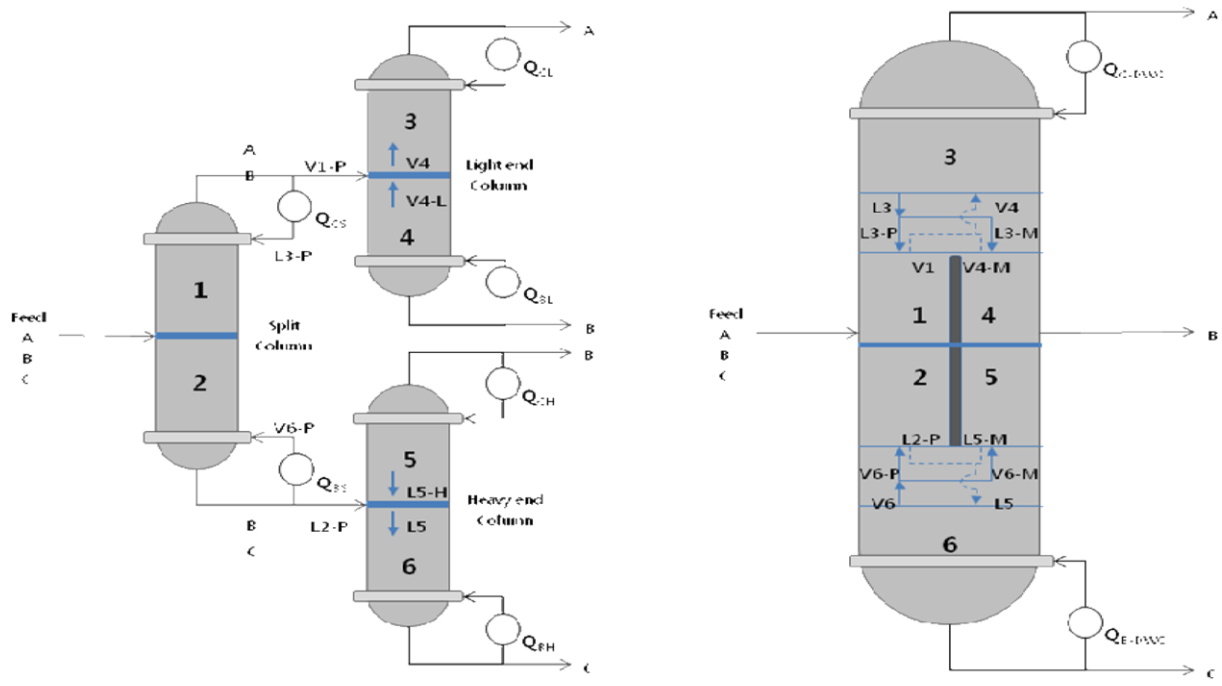

Fig. 1. Schematic diagram of the sloppy column configuration and DWC.

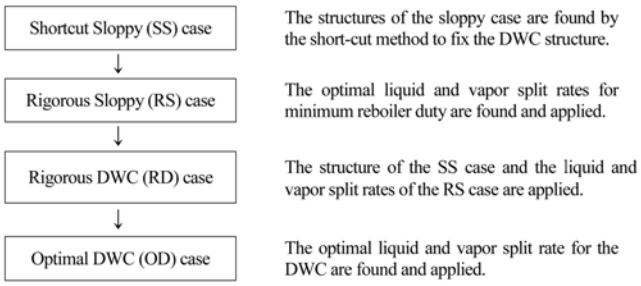

Fig. 2. Four cases used in the analysis.

ske-Underwood-Gilliland method [24,25] was employed to obtain structural details of each column in the sloppy configuration.

DESIGN AND ANALYSIS OF COLUMN STRUCTURE

To investigate the effects of column configuration and simulation rigorousness on DWC design, the four cases as shown in Fig. 2 were designed for analysis: (1) a shortcut sloppy case; (2) a rigorous sloppy case; (3) a rigorous DWC case; (4) an optimal DWC case.

In the shortcut sloppy (SS) case, the sloppy column configuration was considered. The structure of each column was determined by using the well known Fenske-Underwood-Gilliland method:

$$\frac{N-N_m}{N+1}=0.75\left[1-\left(\frac{R-R_m}{R+1}\right)^{0.5688}\right],$$

where the minimum number of theoretical stages at total reflux (N_m) was estimated by the Fenske equation [26] and the minimum reflux for an infinite number of theoretical equilibrium stages (R_m) by the Underwood equation [27]. In this study, the actual reflux ratio (R) was chosen as $1.2R_m$.

The feed tray location was determined by assuming that the relative feed location was constant as the reflux ratio changed from total reflux to a finite value:

$$N_F=\frac{N_{F,m}}{N_m},$$

where $N_{F,m}$ denotes the feed stage at the total reflux estimated by the Fenske equation as:

$$N_{F,m}=\frac{\ln\left[\left(\frac{x_{D,LK}}{x_{D,HK}}\right)\Big/\left(\frac{x_{F,LK}}{x_{F,HK}}\right)\right]}{\ln\alpha_{LK-HK}}.$$

For the design structure of each column in the SS case, possible combinations of the four design variables (the LK specification of the split column bottom; the HK specification of the split column distillate; the LK specification of the light end column bottom; the HK specification of the heavy end column distillate) were searched to fulfill the purity specifications of products A, B, and C. Therefore, there exist hundreds of possible feasible specification sets to meet a given product specification, and accordingly, hundreds of corresponding column structure sets.

In the rigorous sloppy (RS) case, the sloppy configuration was rigorously simulated using the structure obtained from the SS case. The optimal internal flow traffics were found to give a minimum total reboiler duty by changing both the reflux rate and the boil-up rate of the split column for the given purity specifications of products A, B, and C in the light end and heavy end columns.

In the rigorous DWC (RD) case, the DWC was rigorously simulated using the equivalent DWC structure obtained from the corresponding SS case. The liquid and the vapor split rate fed to the prefractionation section were fixed by those obtained from the corresponding RS case.

In the optimal DWC (OD) case, the DWC was rigorously simulated for finding the optimal liquid and vapor split rate into the dividing wall section for minimum energy consumption. The column structure was fixed with those of the corresponding SS case.

SIMULATION STUDY

Nine different feed mixtures were analyzed to investigate the effects of feed composition and relative volatilities of the feed mixtures. Three feed compositions were considered to investigate the effects of feed composition: a mixture with low amounts of the intermediate component (F1); an equimolar mixture (F2); and a mixture with high amounts of the intermediate component (F3). Three mixtures were also considered to assess the effects of relative volatilities in terms of the ease of Tedder and Rudd's separability index (ESI), ESI=$\alpha_{A-B}/\alpha_{B-C}$ [28]. By its definition, if ESI<1, the A/B split is harder than the B/C split; if ESI>1, the A/B split is easier than the B/C split. The mixtures were chosen based upon those studied by Jimenz et al. [29] and are listed in Table 1. The specifications of

Table 1. Feed mixtures used in the simulation study

	Mixture	F1	F2	F3
M1 ESI=1.04	A: *n*-Pentane B: *n*-Hexane C: *n*-Heptane			
M2 ESI=1.86	A: *n*-Butane B: *i*-Pentane C: *n*-Pentane	A: 0.4 B: 0.2 C: 0.4	A: 0.33 B: 0.33 C: 0.33	A: 0.2 B: 0.6 C: 0.2
M3 ESI=0.47	A: *i*-Pentane B: *n*-Pentane C: *n*-Hexane			

*1.0 atm, 45 kmol/h, Property fluid package: Peng-Robinson

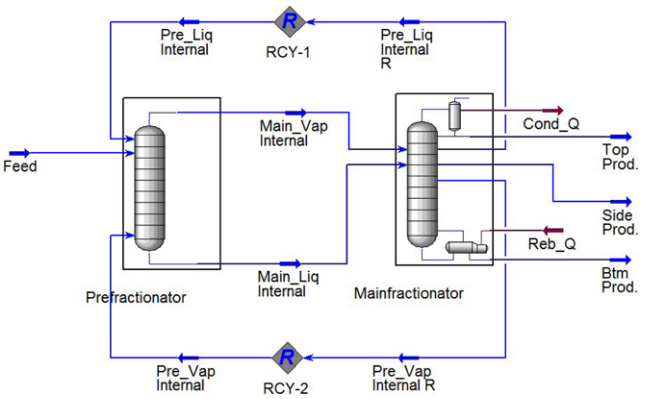

Fig. 3. Process flow diagram of the DWC in HYSYS™.

product purity were selected as 98, 98.5, and 98% for the distillate, intermediate, and bottom products, respectively.

The process simulator HYSYS™ was employed for simulation and design of all cases. For implementation of the DWC in the HYSYS™ environment, the Petlyuk column configuration was used since it is thermodynamically equivalent to the DWC. The resulting process flow diagram of the DWC for the HYSYS™ simulation is shown in Fig. 3.

CONSISTENCY OF DESIGN STRUCTURE

To fix the DWC structure in the initial SS stage, it is highly desirable that the column structure for small energy consumption in the SS case consistently gives small energy consumption in the corresponding DWC, too. Furthermore, the relative energy efficiency among the individual structures has to be not modified by simulation rigorousness, thermal coupling, and/or optimality of internal flow distribution.

Fig. 4 compares the total reboiler duties of the SS, RS, RD, and OD cases for the F3-M1 feed mixture. In Fig. 4, each structure set was arranged in ascending order with respect to the reboiler duty of the SS case and denoted by the structure set number on the x axis. Since each feasible specification set in the SS case results in a different column structure, each structure set implies a different structure and, accordingly, a different equivalent DWC structure. For a given structure set, the structure is the same or equivalent to each other among the SS, RS, RD, and OD cases. As shown in Fig. 4, a consistent trend of energy efficiency was observed for the four different cases; the structure with superior energy efficiency in the SS case is also most likely to bring superior energy efficiency in the other three cases. For example, structure set 1 that shows the best performance in the SS case consistently gave superior energy efficiency for the RS, RD, and OD cases, while structure set 18 yielded an inferior energy efficiency in all four cases. This indicated that in the F3-M1 feed mixture case, once the structure was fixed in the SS stage, the relative energy efficiency among the individual structures did not largely depend on other factors such as simulation rigorousness, thermal coupling, and/or optimality of internal flow distribution.

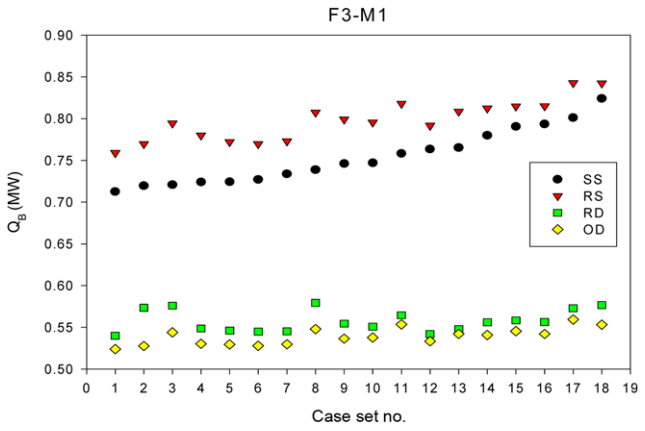

Fig. 4. Consistency of relative energy efficiency between various structures in the sloppy and DWC configurations for the F3-M1 feed case. *SS: Shortcut Sloppy RS: Rigorous Sloppy RD: Rigorous DWC OD: Optimal DWC.

The optimal internal liquid and vapor traffics for the minimum energy consumption in the DWC are likely to be different from those evaluated in the equivalent sloppy configuration. However, as seen in Fig. 4, in the F3-M1 mixture the reboiler duties of the RD and OD are quite close to each other, indicating that the optimal liquid and vapor split rates obtained from the sloppy configuration can also be directly applied to the optimal DWC design. The above similarity in energy consumptions between the RD and OD cases results from either or both reasons: 1. As the structural similarity dominates, the optimal internal flow traffics in the DWC become closer to that obtained from the sloppy configuration, which results in a

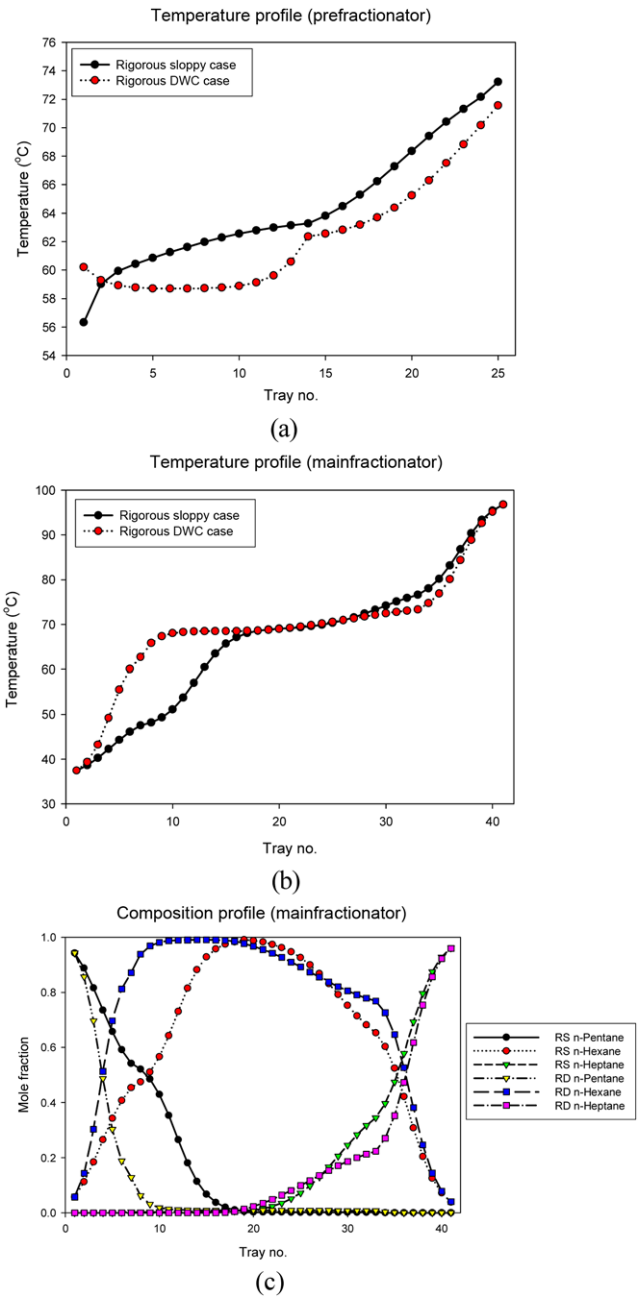

Fig. 5. (a) Temperature profile (prefractionator); (b) Temperature profile (main); (c) Composition profile (Main).

small difference in the reboiler duty between the RD and OD cases; 2. Both the optimal internal flow traffics in the DWC and in the sloppy configuration are in the flat region of the energy contour map where energy consumption remains insensitive to internal traffics.

Structural similarity can also be confirmed from similarity in the temperature (or composition) profiles between the two configurations. Fig. 5 compares the temperature and composition profiles of the RS and the RD cases for the F3-M1 feed mixture. Similarity in the profiles in Fig. 5 also implies the validity of the structural similarity between the sloppy and DWC configurations.

To investigate the consistency of the design structure for various feed mixture cases, the analysis done for the F3-M1 feed was also carried out for other feed mixture cases. Fig. 6 illustrates the total reboiler duties of the SS, RS, RD, and OD cases for the nine feed mixture cases. The figure shows that the optimal DWC design is not very sensitive to the structure set for all nine feed mixture types. Once the internal flows were optimized, the reboiler duty of the DWC was not much different from other DWCs of different structures, implying the optimal structure obtained from the SS case can be satisfactorily applied to the DWC design structure.

It can be also seen that the relative energy efficiency trend for the structure set in the RS case is similar to that in the SS case and indicates that for the ideal mixture, the optimal structure obtained from the SS case can be extended to the rigorous sloppy configuration.

Nevertheless, the relative energy efficiency trend for the four different cases depends on the feed mixture type. As seen in Fig. 6, for the F1-M1, F2-M1, and F3-M1 feed mixtures, the reboiler duties of the RD and the OD cases are very close to each other. Therefore, the optimal internal traffics estimated from the RS case can be reasonably used as those for the optimal DWC design, without resulting in a big loss of energy efficiency. Conversely, the F3-M2 and the F3-M3 feed cases still show a relatively consistent trend in energy efficiency, but the reboiler duty between the RD and OD cases shows a certain gap between each other. The F1-M2, F2-M2, F1-M3, and F2-M3 feed mixtures show no consistent trend in energy efficiency between the RD and the other three cases. In the M2 and M3 mixtures, the required reboiler duty of the RD case is much higher than that of the OD. This can be explained in terms of the energy contour shape and relative location of the optimal internal flow conditions in the DWC, as will be discussed later.

SENSITIVITY AND OPTIMALITY OF DWC DESIGN STRUCTURE

Extensive simulation studies were carried out to investigate the

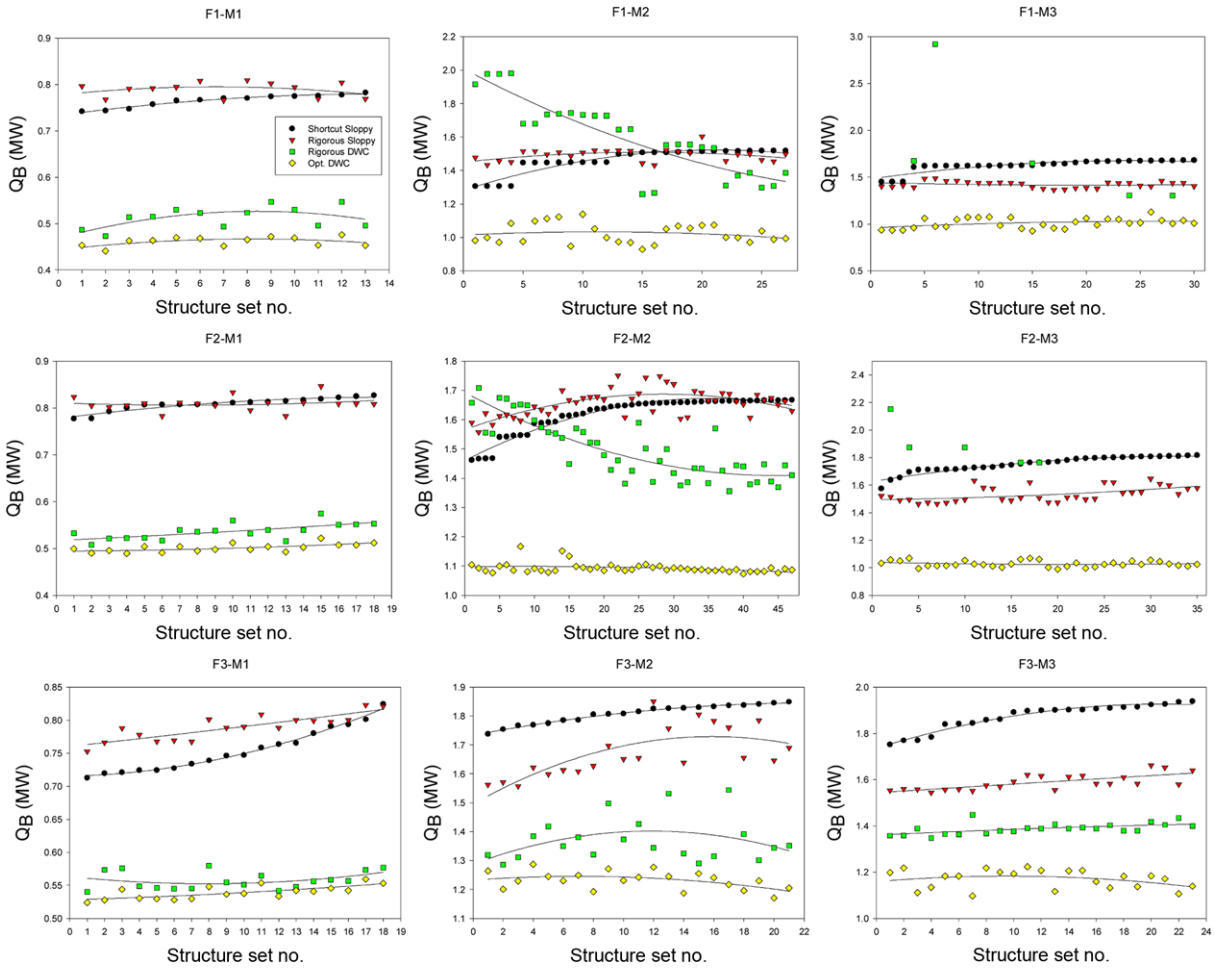

Fig. 6. Consistency of relative energy efficiency between various structures in the sloppy and DWC configurations for the nine feed mixture cases.

Table 2. Structure conditions used for the sensitivity study

	No. of trays in mainfractionator	No. of trays in prefractionator	DW section and location	Feed stream location	Side stream location	Q_B (MW)
Base case	38	15	Top-end: 5 Bottom-end: 33	8	19	0.449
Case study	38	12/15/18	Top-end: 2/5/8 Bottom-end: 29/31/33/35/37	5/8/11	16/19/22	

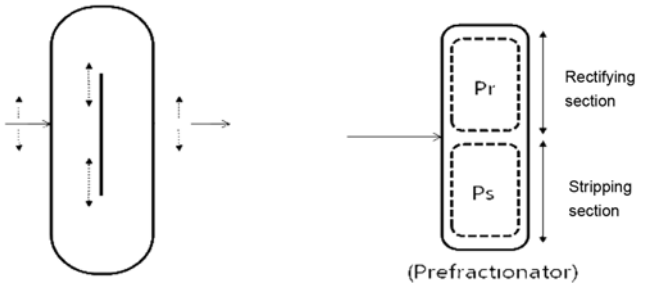

Fig. 7. Structure changes for the sensitivity study.

sensitivity and optimality of the DWC structure obtained from the SS case. Based upon the optimal DWC structure obtained from the SS case, the design variables associated with the structure were randomly changed around the base structure case with every possible combination in a selected range. For example, in the F3-M1 mixture, the divided wall section size and location, prefractionator size, feed, and side stream location were varied in the range listed in Table 2, while the total number of trays in the mainfractionator was fixed with that of the base case. Fig. 7 shows what part of the structure was changed for the sensitivity study. A total of 45 structure sets were tested. For each structure set tested, the internal traffic conditions were optimized and the reboiler duty calculated under optimal internal traffic conditions for a given structure. The result of the reboiler duty for each structure set tried is shown in Fig. 8.

In Fig. 8, the structure set number (denoted by data numbers 1 to 45) indicates the corresponding structure conditions with a different divided wall section size and location, as listed in Table 3. In Table 3, for example, DW:2-37 and Side:16 denote that the dividing wall section is located through tray number 2 and 37 and the side stream at tray number 16 in the mainfractionator. The legends P_r, P_s, P_{rb}, and P_{sb} in Fig. 8 denote the size of the rectification and stripping section in the prefractionator for the trial and base cases, respectively.

In Fig. 8, several structure sets show significantly large reboiler duties while most of the structure sets attempted have similar amounts of reboiler duties. For example, the structure sets 1, 6, 11, 16, 21, 26, 31, 36, and 41 show significantly large reboiler duties compared with other structure sets. All these structure sets are com-

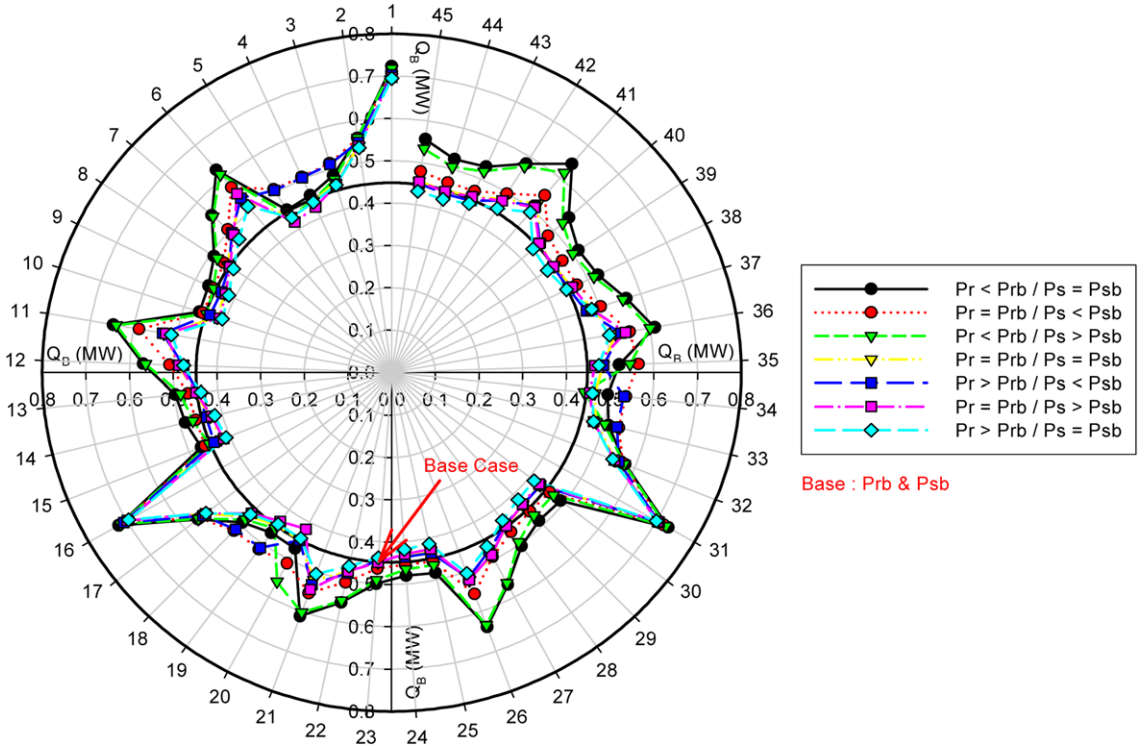

Fig. 8. Radar plot of the reboiler duty for various internal structures with optimized internal traffics.

Table 3. Condition of structure set number in the radar plot

1	DW:2-37/Side:16	10	DW:5-29/Side:16	19	DW:2-31/Side:19	28	DW:8-33/Side:19	37	DW:5-35/Side:22
2	DW:2-35/Side:16	11	DW:8-37/Side:16	20	DW:2-29/Side:19	29	DW:8-31/Side:19	38	DW:5-33/Side:22
3	DW:2-33/Side:16	12	DW:8-35/Side:16	21	DW:5-37/Side:19	30	DW:8-29/Side:19	39	DW:5-31/Side:22
4	DW:2-31/Side:16	13	DW:8-33/Side:16	22	DW:5-35/Side:19	31	DW:2-37/Side:22	40	DW:5-29/Side:22
5	DW:2-29/Side:16	14	DW:8-31/Side:16	23	DW:5-33/Side:19	32	DW:2-35/Side:22	41	DW:8-37/Side:22
6	DW:5-37/Side:16	15	DW:8-29/Side:16	24	DW:5-31/Side:19	33	DW:2-33/Side:22	42	DW:8-35/Side:22
7	DW:5-35/Side:16	16	DW:2-37/Side:19	25	DW:5-29/Side:19	34	DW:2-31/Side:22	43	DW:8-33/Side:22
8	DW:5-33/Side:16	17	DW:2-35/Side:19	26	DW:8-37/Side:19	35	DW:2-29/Side:22	44	DW:8-31/Side:22
9	DW:5-31/Side:16	18	DW:2-33/Side:19	27	DW:8-35/Side:19	36	DW:5-37/Side:22	45	DW:8-29/Side:22

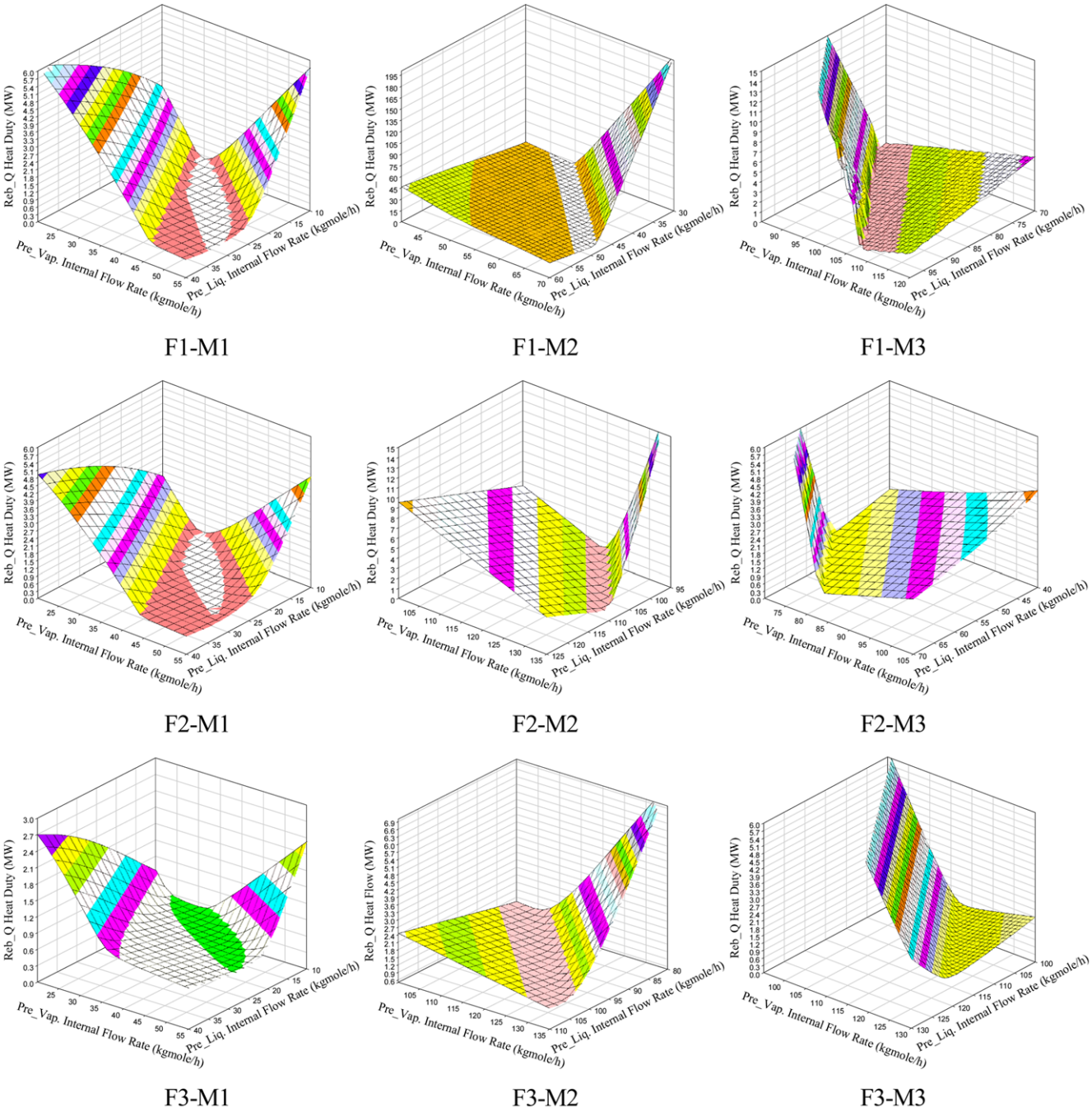

Fig. 9. Effects of internal flow distribution on the energy consumption in DWC.

monly characterized with a bottom end of the divided wall being located at the excessively low bottom section (tray no. 37). Especially, the structure sets 1, 16, and 31, where the top end of the divided wall is also located at the excessively high top section (tray no. 2), showed the largest duties regardless of the size and internal structure of the prefractionator. The excessively low (or high) location of the divided wall leads to a lack of a necessary number of trays for proper stripping (or proper rectifying) in the main section of the DWC. This, in turn, results in higher energy for securing the required bottom and/or distillate product purity specification. Except for those structure sets where the divided wall was located at the extreme top or bottom section, the energy efficiency of the DWC remained fairly insensitive to structural changes. Furthermore, the optimal structure obtained from the SS case, the base case structure, belonged to the structure set group, giving a minimum reboiler duty. It also indicated that the near-optimal DWC structure can be satisfactorily determined by the sloppy configuration in the initial design stage.

SENSITIVITY AND OPTIMALITY OF INTERNAL FLOW DISTRIBUTION

Fig. 9 shows the effect of internal flow distribution on the energy consumption in the DWC for the nine feed mixture cases and clearly illustrates the existence of an optimal internal flow distribution that generates the lowest energy consumption. The figure also indicates that the energy consumption is largely affected by the internal flow distribution. Generally, the internal liquid and vapor flows into the prefractionator and main dividing wall section are the most crucial design factors affecting overall energy consumption and separation efficiency among all the design variables.

As seen in Fig. 9, all the M1 cases show a wide and flat symmetrical distribution of the required energy contour, in which the energy efficiency is not significantly affected by the internal flow changes around the optimal internal flow conditions. The optimal internal flow condition from the RD case is also possibly located on the flat area in the energy consumption contour map. However, the M2 and M3 cases show a narrow and stiff unsymmetrical shape in the energy consumption contour. Therefore, the energy efficiency in the M2 and M3 cases can be drastically deteriorated by a small deviation in the internal flows from the optimal conditions, depending on the direction of the deviation from the optimal conditions. This sensitivity of internal traffics to the energy efficiency is closely related to the ESI characteristic and accordingly to the DWC structure. As the ESI is closer to 1 (the M1 case), the divided wall is designed to be located around the middle of the mainfractionator. As a result, the composition distribution of the intermediate component becomes symmetrical along the column and evenly affected by positive and negative changes in the internal flows from the optimal value. For a feed mixture with an ESI value away from 1, the optimal location of the divided wall tends to be located either at the top or bottom section. Thus, any change in the internal flows from optimal conditions can have a sensitive and unsymmetrical effect on energy effi- ciency.

CONCLUSIONS

Extensive simulation studies were carried out with a thorough analysis to investigate the DWC design for various types of ideal feed mixtures. The feed mixture was characterized in terms of ESI and feed composition. As a result, the following conclusions were obtained:

- The optimal DWC structure can be reasonably determined by the optimal structure of the corresponding sloppy configuration using the proposed shortcut design structure method.
- The energy efficiency of the DWC is not very sensitive to the structural changes around the optimal structure. However, in the case where the divided wall is located in excess at the top or bottom sections, the energy efficiency is sensitive to structural changes.
- The internal flow distribution is the most dominant design variable influencing the energy efficiency of the DWC. In general, the optimal internal flows for the DWC cannot be directly estimated from the RS configuration. However, for the M1 feed mixture cases, the optimal internal flow from the sloppy configuration can be satisfactorily applied towards determining the optimal internal flows of the corresponding DWC. For the M2 and M3 feed mixture cases, direct application of the optimal internal flow conditions from the sloppy configuration can result in significant deterioration in the energy efficiency of the corresponding DWC.

Based on the analysis, a two-step approach is suggested for the optimal design of the DWC: the structure of the DWC is designed using the optimal structure from the corresponding shortcut sloppy configuration; the optimal internal flow conditions are then directly determined from the DWC configuration.

ACKNOWLEDGEMENTS

We appreciate the financial aid for this study from the KETEP 2009.

REFERENCES

1. K. P. Yoo, K. S. Lee, W. H. Lee and H. S. Park, *Korean J. Chem. Eng.*, **5**(2), 123 (1988).
2. M. L. Zaki and E. S. Yoon, *Korean J. Chem. Eng.*, **6**(3), 185 (1989).
3. K. A. Amminudin and R. Smith, *Trans. Inst. Chem. Eng.*, **79** Part A, 716 (2001).
4. Y. H. Kim, *Korean J. Chem. Eng.*, **17**(5), 570 (2000).
5. I. J. Halvorsen and S. Skogestad, *Ind. Eng. Chem. Res.*, **42**, 605 (2003).
6. I. J. Halvorsen and S. Skogestad, *Ind. Eng. Chem. Res.*, **43**, 3994 (2004).
7. Y. H. Kim, M. Nakaiwa and K. S. Hwang, *Korean J. Chem. Eng.*, **19**(3), 383 (2002).
8. Y. H. Kim, *Chem. Eng. J.*, **85**, 289 (2002).
9. M. A. Phipps and A. F. A. Hoadley, *Korean J. Chem. Eng.*, **20**(4), 642 (2003).
10. I. P. Nikolaides and M. F. Malone, *Ind. Eng. Chem. Res*., **27**, 811 (1988).
11. A. L. Querzoli, A. F. A. Hoadley and T. E. S. Dyson, *Korean J. Chem. Eng.*, **20**(4), 635 (2003).
12. R. Agrawal, *Trans. Inst. Chem. Eng*., **78** PartA, 454 (2000).
13. Y. H. Kim, D. W. Choi and K. S. Hwang, *Korean J. Chem. Eng.*, **20**(4), 755 (2003).
14. Y. H. Kim, K. S. Hwang and M. Nakaiwa, *Korean J. Chem. Eng.*,

21(6), 1098 (2004).
15. J. G. Segovia-Hernandez, A. Bonilla-Petriciolet and L. I. Salcedo-Estrada, *Korean J. Chem. Eng.*, **23**(5), 689 (2006).
16. M. Y. Lee and Y. H. Kim, *Korean Chem. Eng. Res.*, **46**(5), 1017 (2008).
17. M. Y. Lee, S. Y. Jeong and Y. H. Kim, *Korean J. Chem. Eng.*, **25**(6), 1245 (2008).
18. M. Y. Lee, D. W. Choi and Y. H. Kim, *Korean J. Chem. Eng.*, **26**(3), 631 (2009).
19. K. S. Hwang, I. G. Sung and Y. H. Kim, *Korean Chem. Eng. Res.*, **47**(3), 327 (2009).
20. C. Triantafyllou and R. Smith, *Trans. Inst. Chem. Eng.*, **70**, Part A, 118 (1992).
21. K. A. Amminudin, R. Smith, D. Y. C. Thong and G. P. Towler, *Chem. Eng.*, **85**, 289 (2002).
22. R. Agrawal and Z. T. Fidkowski, *AIChE J.*, **45**, 485 (1999).
23. R. Premkumar and G. P. Rangaiah, *Chem. Eng. Res. Des.*, **87**, 47 (2009).
24. M. R. Fenske, *Ind. Eng. Chem.*, **32** (1932).
25. E. R. Gilliland, *Ind. Eng. Chem.*, **32**, 1220 (1940).
26. M. R. Fenske, *Ind. Eng. Chem.*, **24**, 482 (1932).
27. A. J. Underwood, *Chem. Eng. Progress.*, **44**, 603 (1948).
28. D. W. Tedder and D. F. Rudd, *AIChE J.*, **24**, 303 (1978).
29. A. Jiménez, N. Ramírez, A. Castro and S. Hernández, *Trans. Inst. Chem. Eng.*, **81**(A5), 518 (2003).
30. E. A. Wolff and S. Skogested, *Ind. Eng. Chem. Res.*, **34**(6), 2094 (1995).
31. I. J. Halvorsen and S. Skogestad, *J. Process Control*, **9**(5), 407 (1999).
32. M. I. Abdul Mutalib, A. O. Zeglam and R. Smith, *Trans. Inst. Chem. Eng.*, **76**(A3), 308 (1998).